Proceedings of the International Conference on Heat Transfer and Fluid Flow
Prague, Czech Republic, August 11-12, 2014
Paper No. 200

Vertical Wall with Tilted Cavities Used as a Thermal Diode: Scale Analysis Describing its Performance

Louis Gosselin
Department of Mechanical Engineering, Université Laval
1065, avenue de la Médecine, Québec City, QC, Canada
Louis.Gosselin@gmc.ulaval.ca

Alexandre Kupka da Silva
Universidade Federal de Santa-Catarina, Engenharia da Energia
Rua Pedro João Pereira, 150, Araranguá, SC, Brasil
alexandrekupka@gmail.com

Abstract – In this paper, we analyse the heat transfer and fluid flow in tilted cavities sandwiched between two vertical parallel plates. Such a wall could be used as thermal diode to promote heat in one direction, and block it in the other. We present a scale analysis to determine the average heat flux as a function of the cavity aspect ratio and tilt angle, as well as the Rayleigh number. The scaling is compared with CFD results and shows satisfactory results. A comparison between the forward and reverse modes is provided in the paper. A convenient representation of the wall as a diode network allows further simulations and optimization on in which such walls would be integrated into more complex systems such as buildings.

***Keywords*:** Tilted cavities, Natural convection, Thermal diodes, Scale analysis.

1. Introduction

Diodes used in electrical circuits can either allow the current to pass when a positive voltage drop is applied, or block it when the voltage drop is negative. A similar behavior is encountered in different thermal systems, in which heat transfer can be either promoted or inhibited (i.e. forward versus reverse modes) depending on the direction of the imposed temperature difference, thus yielding to the concept of "thermal diodes".

Thermal diodes can be included in thermal circuit models, which is convenient for building simple models of complex systems. They show up in a wide variety of applications: road engineering (Chataigner et al., 2009), renewable energy (Chaudhry et al., 2012), buildings solar walls (Albanese et al., 2012), thermal storage systems (Shabgard et al, 2010), etc.

Different types of thermal diodes are possible. In particular, in the last years, efforts have been devoted to improve heat pipe designs, in which a fluid evaporates at the hot side of the heat pipe, raises to the cold side due to buoyancy forces, condenses and returns to the hot side by gravity or capillarity (e.g., Li et al., 2010; Ranjan et al., 2011). Solid state thermal diodes are also emerging as a potential technology for heat transfer control (Wang and Wu, 2014; Chang et al., 2006).

Another class of thermal diodes relies on tilted, vertical or horizontal cavities (Bairi et al., 2011). In this paper, we present an analysis of a thermal diode consisting of a vertical wall divided into a series of titled cavities. The advantage of this design compared to other existing thermal diodes is its simplicity and low-cost. However, their performance can be disappointing which call for sound models and design optimization to improve their features.

2. Description of the Problem

A schematic representation of the system that was studied is shown in Fig. 1. Two vertical plates at different temperatures are separated by a distance L. Between these plates, partitions are installed in order to create a series of tilted cavities filled with air. The cavities are characterized by the tilt angle ε and by the cavity height, H. In the present study, the partitions are assumed to be adiabatic.

When a temperature difference is between the two vertical plates, two situations can happen as shown in the right-hand side of Fig. 1. In the configuration of Fig. 1b, a circulation loop is triggered thus promoting heat transfer between the two plates (forward mode). On the other hand, when the temperature difference is reversed as in Fig. 1c, the movement of air is impeded and a thermal stratification takes place in parts of the cavity. The thermal stratified zones are shown in color in Fig. 1c. This second configuration is less performant than the first one in terms of heat transfer (reverse mode).

In order to present the results in a convenient way, the tilt angle of the cavity, ε, was considered as positive in the forward mode, and negative in the reverse mode, as depicted in Fig. 1. In other words, for a given cavity geometry, reversing the applied temperature difference is equivalent to changing the sign of the tilt angle.

In order to characterize the performance of a diode, one must determine its performance in both modes of operation (reverse and forward modes). This performance was characterized by the average heat flux from the hot to the cold wall, which can be expressed with dimensionless variables as

$$\tilde{q}'' = \frac{\overline{q}''}{\left(k\Delta T/L\right)} \tag{1}$$

where k is the air thermal conductivity, $\Delta T = T_H - T_C$, and L is the thickness of the wall (see Fig. 1).

When convection is significant, $\tilde{q}''$ will be larger than 1 since the denominator of Eq. (1) represent the conduction heat flux. For a given wall-to-wall temperature difference, two values of $\tilde{q}''$ will be evaluated, one for each mode of the thermal diode.

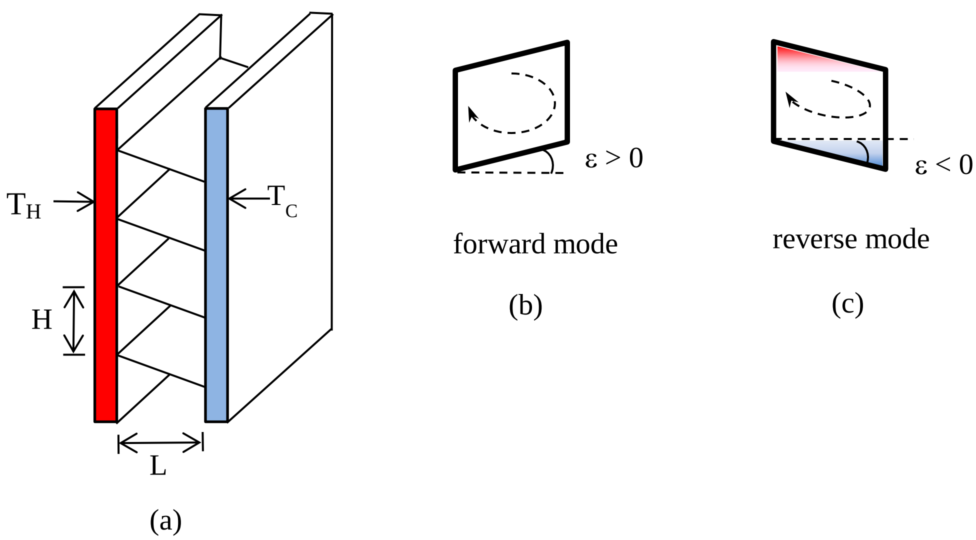

Fig. 1. Schematic representation of a (a) vertical wall containing tilted cavities, (b) forward mode of operation, and (c) reverse mode of operation.

The main assumptions used in this work are: (i) the flow in the cavity is laminar, (ii) the fluid is Newtonian with Pr ~ 1, (iii) the properties are constant, (iv) radiation heat transfer is neglected, (v) the partitions between the cavities are assumed to be adiabatic; (vi) the wall is treated in 2D.

3. Scale Analysis

In this section, a scale analysis is presented in order to predict the behavior of the thermal diode wall system of Fig. 1 in both the reverse and forward modes. This analysis aims at determining the main dependence of the average heat flux, $\tilde{q}''$, as a function of the main governing parameters of this problem. The results of this 'order of magnitude' analysis will be compared to numerical simulations later in this paper.

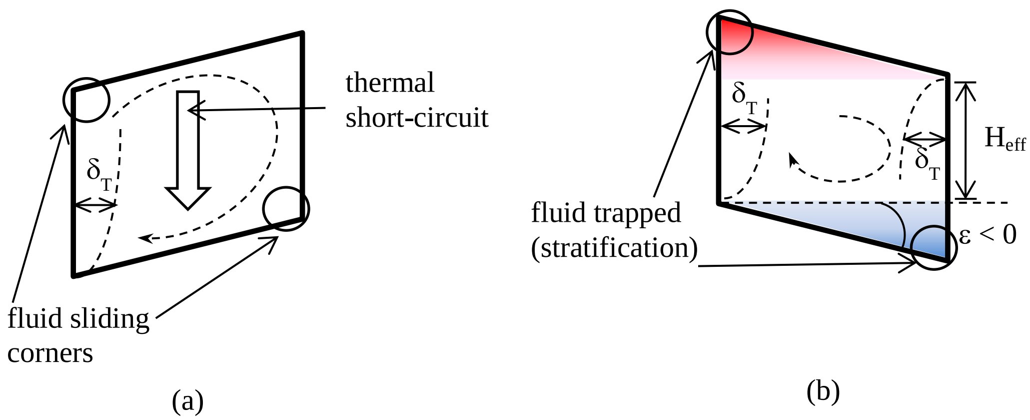

Fig. 2. Illustrated heat transfer mechanisms in the (a) forward mode of operation, and (b) reverse mode of operation.

3.1. Reverse Mode

First, the reverse configuration is considered, i.e. negative values of ε (Fig. 2b). In that case, there are some fluid pockets that stay stagnant due to the stable thermal stratification that occurs naturally in the cavity. As the cavity becomes more and more tilted, the circulation loop shrinks. The effective height of the circulation loop can be estimated by geometrical considerations as revealed by Fig. 2b:

$$H_{eff} \simeq H - L \tan \varepsilon \tag{2}$$

That relation stays valid as long as H_{eff} is above 0, i.e.

$$\frac{H}{L} > \tan \varepsilon \tag{3}$$

The criterion of Eq. (3) defines when a circulation loop exists in the cavity in the reverse mode. It if is not respected, a purely conductive regime prevails. For example, when H/L = 1, the critical tilt angle for the existence of a circulation loop is −45°. More tilted cavities would be purely conductive in nature, but that regime is not covered in this paper.

The average dimensionless heat flux through the wall can be estimated by assuming that the heat is transferred from the hot to cold vertical surface by the circulation loop with its effective height,

$$\overline{q}'' \sim \frac{k\Delta T}{\delta_T} \frac{H_{eff}}{H} \tag{4}$$

where δ_T is the thickness of the thermal boundary layers that grow on the vertical sidewalls, as shown in Fig. 2b. The two vertical boundary layers are assumed to be distinct, so that Eq. (4) is valid. Then, using the correlation δ_T = $0.387\mathrm{Ra}_{H_{eff}}^{-1/4}$ (Bejan, 2003) with the estimation of the effective height, Eq. (4) becomes:

$$\tilde{q}'' \sim 0.387\frac{1}{\tilde{H}^{1/4}}\left(1-\frac{\tan\varepsilon}{\tilde{H}}\right)^{3/4}\mathrm{Ra}_L^{1/4} \quad \text{(reverse mode)} \tag{5}$$

3.2. Forward Mode

In the forward mode, Fig 2a, two vertical boundary layers grow on each vertical plate, but this time, over the entire height H of the cavity. This tends to increase the heat transfer rate. On the other hand, two phenomena act to limit the overall heat exchange. First, the shape of the loop is that of a parallelogram rather than a straight plane. Furthermore, when the tilt angle is high, heat can be transferred from the upper tilted part of the loop to the lower tilted part, thus creating a thermal short circuit, as shown in Fig. 2a. Note that these two effects are also present in the reverse mode. Therefore, Eq. (5) should be seen as the threshold for the possible heat flux in the reverse mode.

Compared to a hypothetical boundary layer growing on a vertical plate only, the velocity in the loop is reduced due to an addition head loss $\Delta P = K\rho V^2/2$, where K is the heat loss coefficient due to a change of direction by an angle (90° − ε). The dynamic pressure created by the buoyancy force that would have generated the vertical boundary layers on the sidewall alone must in reality act to maintain the flow in the presence of additional head loss. This means that the real velocity will be reduced compared to the hypothetical situation of a boundary layer on a flat plate alone:

$$V_{\substack{\text{plate}\\\text{alone}}}^2 \sim V^2\left(1+K\right) \tag{6}$$

The left-hand side term in Eq. (6) is known from boundary layer theory since it corresponds to the classical case of a boundary layer growing on a flat plate (Bejan, 2003), and scales as $\left(\alpha/H\right)\mathrm{Ra}_H^{1/2}$. Therefore, the actual "reduced" velocity taking into account the change of direction of the flow would be of the order of:

$$V \sim \frac{\alpha}{H}\frac{\mathrm{Ra}_H^{1/2}}{\left(1+K\right)^{1/2}} \tag{7}$$

This reduced velocity will increase the boundary layer thickness. Combining Eq. (7) with the expression of the boundary layer just above Eq. (5), one finds:

$$\frac{\delta_T}{H} \sim \frac{\left(1+K\right)^{1/4}}{\mathrm{Ra}_H^{1/4}} \tag{8}$$

And finally, translating the boundary layer thickness in terms of the dimensionless average heat flux, it can be shown that:

$$\tilde{q}'' \sim \frac{\mathrm{Ra}_L^{1/4}}{\tilde{H}^{1/4}\left(1+K\right)^{1/4}} \tag{9}$$

The relation between K and the tilt angle ε could be established by the following proposed fitting:

$$K = K_0 - \left(K_0 + A\right)\left(\frac{\varepsilon}{90}\right) + A\left(\frac{\varepsilon}{90}\right)^2 \qquad (10)$$

where K_0 is the value of K when ε = 0°, and A is a fitting constant. Based on different data for head loss in elbows (McQuiston et al., 2008), it was found that K_0 = 0.8 and A = 0.7 provided satisfactory results. Further research would be required to establish more precisely these constants. Eqs. (10) and (9) reveal that more heat is transferred as ε increases, i.e. as the cavity is more tilted.

From the above discussion, one could think that increasing the tilt of the cavity would constantly enhance the heat transfer in the cavity, and that highly tilted cavities would be preferable. However, an insulating effect is also created by the two oblique jet flows that interact thermally in tilted cavities. The normal distance between the two oblique walls is $H\cos\varepsilon$, and the length of the oblique walls, i.e. the distance travelled by the oblique jets, is $L/\cos\varepsilon$. The thickness of these two jets scales as δ_T. The heat transfer rate exchanged between the two oblique jets is thus of the order of:

$$q'_{\substack{\text{short}\\\text{circuit}}} \sim \left(\frac{k\Delta T}{H\cos\varepsilon - \delta_T}\right)\left(\frac{L}{\cos\varepsilon}\right) \qquad (11)$$

This thermal short-circuit reduces the amount of heat transferred from one wall to another. The actual heat transfer rate of Eq. (9) is reduced by the amount of Eq. (11). It can be shown that the resulting expression for the dimensionless average heat flux in the forward mode is:

$$\tilde{q}'' \sim \left[0.387\left(\frac{Ra_L}{\tilde{H}\left(1+K\right)}\right)^{1/4} - \left(\cos\varepsilon - 0.387\tilde{H}^{-1}\left(\frac{Ra_L}{\tilde{H}\left(1+K\right)}\right)^{-1/4}\right)^{-1}\left(\frac{1}{\tilde{H}^2\cos\varepsilon}\right)\right] \text{ (forward mode)} \qquad (12)$$

4. Numerical Modeling

A numerical model was developed to simulate the heat transfer and fluid flow in tilted cavities. Due to the page limitation, all details are not provided here. The model included the governing equations for the conservation of mass, momentum and energy. Boussinesq approximation was used to account for buoyancy forces. The model was implemented on a commercial finite element solver (Comsol, 2010). Mesh independence was tested to ensure the validity of the results. The model was validated by comparing the results for a straight cavity (i.e., ε = 0°) to existing correlations (T.L. Bergman et al., 2011). Differences were found to be within the uncertainties of the correlations, therefore confirming the validity of the implemented numerical model.

The model was then used to determine the dimensionless average heat flux, Eq. (1), as a function of the Rayleigh number and of the geometry of the cavity, which is characterized by the aspect ratio H/L = $\tilde{H}$ and by the tilt angle ε. The results obtained with the numerical model are compared to the scale analysis in the next section.

5. Results and Discussion

Figure 3 presents the effect of the tilt angle on the heat transfer performance of the cavity, for given values of Ra and $\tilde{H}$. Both the results of the scale analysis (i.e., Eqs. (5) and (12)) and the ones of the numerical simulations are reported in the figure. Note that in the reverse mode, as mentioned previously, some effects decreasing the heat flux have not been taken into account in Eq. (5). It was found empirically that a factor of the order of 0.7 was useful to account for these effects and avoid a discontinuity at $\varepsilon = 0$, i.e. when changing from Eq. (12) to Eq. (5). This factor was used in the figures below.

First, it is worth to mention that the agreement between the scaling and the simulations was found to be quite good, in an order of magnitude sense. The scale analysis was able to capture the most important aspects of this problem and to predict adequately the behavior of the thermal diode.

For negative angles, the heat transfer rate decreases as the cavity becomes more tilted. As mentioned above, this is caused by the gradual reduction of the circulation loop within the cavity and the creation of stagnant stratified zones. On the other hand, for positive tilt angle, the heat transfer rate starts by increasing and then decreases as the tilt angle is increased. In other words, the heat transfer rate reaches a maximum. In the present case, this maximum occurs around an angle of 15°. The occurrence of this maximum is due to the competing presence of a thermal short-circuit between the two oblique jets described above and the head loss in the corners of the cavity.

Figure 4 presents the information of Fig. 3 in a slightly different way, which is more appropriate in the context of a thermal diode application. The heat flux in both modes for a given tilt angle, i.e. $\tilde{q}''$ for $\pm\varepsilon$ (forward and reverse modes), is reported in Fig. 4a. In Fig. 4b, the ratio of the reverse heat flux over the forward heat flux is shown as a function of the tilt angle. Obviously, when $\varepsilon = 0$, both modes are equivalent as the cavity is not tilted. As the tilting is increased, the differentiation between both modes becomes more and more stringent. For example, at $\varepsilon = 30°$, the heat flux ratio is around 50%, which means that the heat transfer rate is about twice as large in the forward than in the reverse mode. However, it should also be pointed that, overall, the heat transfer rate tends to decrease at higher angle even in the forward mode, compared to less tilted cavities. Therefore, depending on the application considered, the tilt angle should be selected appropriately.

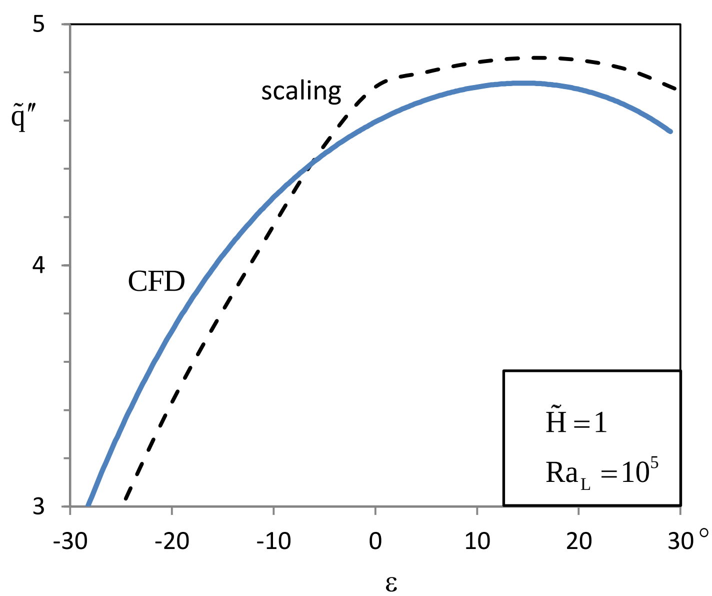

Fig. 3. Dimensionless heat transfer rate as a function of the tilt angle for $Ra = 10^5$ and $\tilde{H} = 1$.

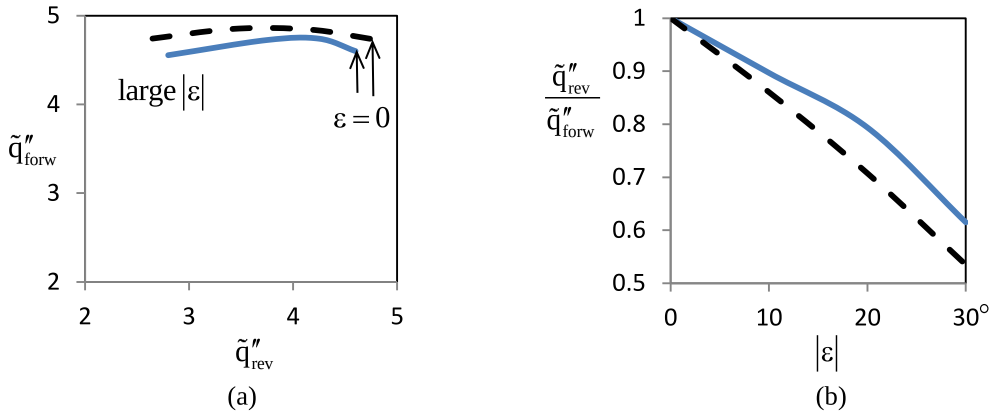

Fig. 4. Dimensionless heat transfer rate as a function of the tilt angle for Ra = 10^5 and $\tilde{H}$ = 1, (a) forward versus reverse heat flux, and (b) heat flux ratio as a function of the tilt angle.

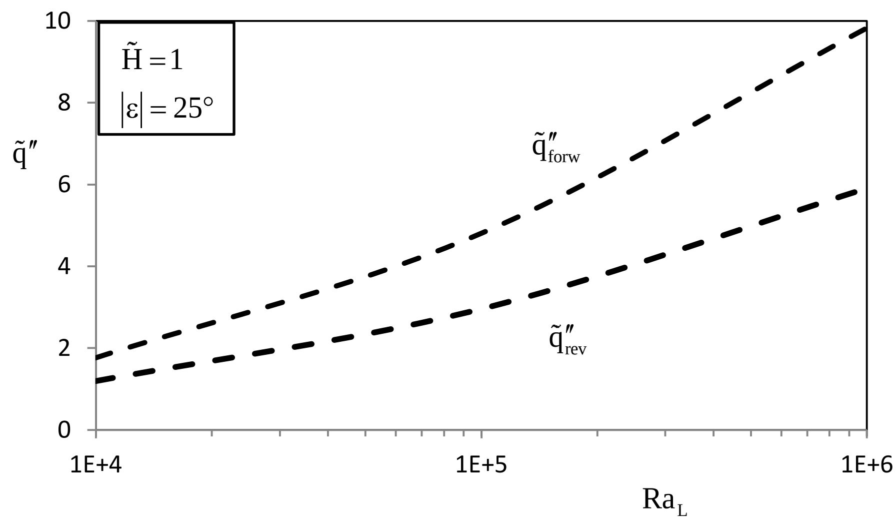

Fig. 5. Dimensionless heat transfer rate as a function of Ra for a tilt angle ε = 25° and aspect ratio $\tilde{H}$ = 1.

The effect of the Rayleigh number was also investigated. It was observed that the heat transfer rate tends to increase with Ra, since buoyancy forces are more important at high Ra. Also, the value of the tilt angle at which the heat transfer rate is maximal increases with Ra. This is obtained both by the numerical simulations and the order of magnitude analysis. A plateau is observed for low ε-values in the forward mode, i.e. that the heat transfer rate varies only slightly with the tilt. It is also interesting to note that the diode effect is more stringent at high Ra. However, there is a diminishing return effect: above a certain value of Ra, there is no more gain in terms of the reverse/forward heat flux ratio. Figure 5 reports an example of results, i.e. the forward and reverse heat flux as a function of Ra.

Finally, the thermal wall studied in this paper can be represented by the thermal circuit of Fig. 6. In the representation that is proposed, when $T_1 > T_2$, heat will flow through the surface resistance R''_{rev} , whereas when the applied temperature difference is the other way around, heat will flow in the resistance R''_{forw}. The resistance R''_{forw} is larger than R''_{rev}. Each of these resistances depend on shape of the cavity (i.e., ε and $\tilde{H}$), and also on the temperature difference through the Rayleigh number. The system of Fig. 6 could be combined to other thermal network.

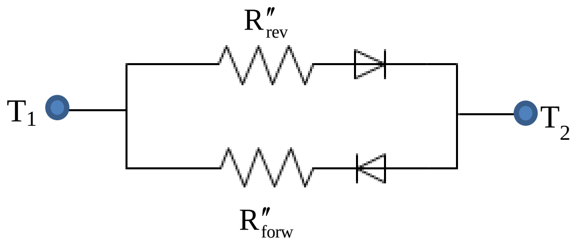

Fig. 6. Diode representation of the wall with cavities.

6. Conclusions

A scale analysis is presented, and validated with CFD simulations, to determine the average heat flux in a vertical wall composed of tilted cavities. The wall is considered as a thermal diode, enhancing heat transfer in one direction, and blocking it in the other direction. The effects of the cavity geometry and of the Rayleigh number are presented. A convenient network representation is proposed to model the system.

More work is required to validate further the model (e.g., to account for effect of the cavity aspect ratio). Some of the assumptions could be released in future work. For example, considering radiation could be interesting in different applications.

Finally, this work will allow to develop tool to simulate and optimize larger systems in which such walls are to be used.

Acknowledgements

Gosselin’s work is supported by the Natural Sciences and Engineering Research Council of Canada (NSERC).

References

Albanese M.V., Robinson B.S., Brehob E.G. et al. (2012). Simulated and experimental performance of a heat pipe assisted solar wall. Solar Energy, 86, 1552-1562.

Bairi A., Zarco-Pernia E., Garcia de Maria J.-M. et al. (2011). Nusselt-Rayleigh correlations for free convection in 2D air-filled parallelogrammic enclosures with isothermal active walls. Heat and Mass Transfer, 47, 589-595.

Bejan, A. (2003) “Convection Heat Transfer” 3rd Edition Wiley.

Chataigner Y., Gosselin L.; Dore G. (2009) Optimization of embedded inclined open-ended channel in natural convection used as heat drain . Int. J. Thermal Sciences, 48, 1151-1160.

Chang C.W., Okawa D., Majumdar A. et al. (2006). Solid-state thermal rectifier. Science, 314, 1121-1124.

Chaudhry H.N., Hughes B.R., Ghani S.A. (2012). A review of heat pipe systems for heat recovery and renewable energy applications. Ren. & Sustainable Energy Reviews, 16, 2249-2259.

COMSOL Multiphysics 4.2, 2010.

Li J., Wang D., Peterson G. P. (2010). Experimental studies on a high performance compact loop heat pipe with a square flat evaporator. Applied Thermal Engineering, 30, 741-752.

McQuiston et al. (2008) “Heating, Ventilating, and Air Conditioning - Analysis and Design” 6th Ed. Wiley.

Ranjan R., Murthy J.Y.; Garimella S.V. et al. (2011). A numerical model for transport in flat heat pipes considering wick microstructure effects. Int. J. Heat Mass Transfer, 54, 153-168.

Shabgard H., Bergman T.L., Sharifi, N. et al. (2010) High temperature latent heat thermal energy storage using heat pipes. Int. J. Heat Mass Transfer, 53, 2979-2988.

Wang L., Wu J. (2014). Frequency response of a thermal diode. Physical Review E, 89, 012119.